

Growth and Characterization in Vitro Antimicrobial Activity of Oxalic Acid -Derived Copper Complex of Non Linear Optical Crystal

F. Daisy Selasteen¹, S. Alfred Cecil Raj², R. Jeba Kumar Pandian¹, S. Iniyan¹
M. Uma¹

¹P. G and Research Department of Physics, Bishop Heber College, Tiruchirappalli, TamilNadu, India.

²School of Physics, St. Joseph's College, Tiruchirappalli, TamilNadu, India.

Corresponding Author: F. Daisy Selasteen¹

Abstract: Sodium Copper Oxalate $\text{Na}_4\text{Cd}_2(\text{C}_2\text{O}_4)_4\cdot 4\text{H}_2\text{O}$ (NaCuOx) single crystal was grown as transparent crystal using single diffusion silica gel technique. The triclinic and centrosymmetric nature of NaCuOx crystal structure with the P-1 space group was determined by the powder x-ray diffraction method. The functional groups were identified by FTIR spectroscopy. TGA of NaCuOx showed the formation of stable metal oxide at various temperatures due to the decomposition of ligand moieties. The projected optical parameters of the NaCuOx crystal were calculated by the UV-Vis-NIR and the highest absorption peak observed from the photo luminescence emission spectrum was used to explore the nonlinear optical efficiency of the as-grown crystal. The first attempt on antimicrobial activity of this crystal was carried at different concentrations (25, 50, 75 and 100 mg/ml) in-vitro against *Aspergillus Niger* (fungus); *Escherichia coli* (G-Ve) microbial strains. These studies established that NaCuOx crystals might find useful applications in the field of biomedical and nonlinear optics.

Keywords: $[\text{Na}_4\text{Cu}_2(\text{C}_2\text{O}_4)_4\cdot 4\text{H}_2\text{O}]$ crystal growth from gel, Optical material, Thermal stability, Antimicrobial Activity

Date of Submission: 29-08-2018

Date of acceptance: 13-09-2018

I. Introduction

The oxalate compound is engaged in constructing a large variety of molecular structures and frameworks by incorporating suitable metal ions in the crystal lattice. It can act as a mono dentate, bidentate, tridentate or tetra dentate donor ligand and can form chains, layers or three-dimensional networks with metal centers. Outstandingly, oxalate is often encountered as a bidentate, chelating ligand ($\text{C}_2\text{O}_4^{2-}$), for metal cations. The combination of alkali mixed heavy metal elements with oxalate ions forms new compounds which are scientifically and technologically interesting and deserve special attention because of their many interesting structural, spectral, luminescent and optical [1,2] properties which are utilized widely in their use in transducers and optoelectronic industries [3].

Oxalic acid is a natural chemotherapy void of troubling side effects and is a usual element in human blood and must be accessible for the immune system to fight against the diseases of cancer, viral, bacterial and vascular conditions. It has a mean value of 288 mg of anhydrous oxalic acid/ 100 ml of blood. When it falls below an effective level the immune system can no longer protect the body from various diseases [4].

In the body, oxalic acid combines with divalent (Cd^{2+}) metals to form crystals of the corresponding oxalates, which are then excreted in urine as minute crystals. The use of an oxalate to bind with a metal (as Fe, Na, Cd, Zn, and Cu) in the body to form a chelate so that the metal loses its toxic effect or physiological activity. In the metal oxalates, mainly atoms like C and O function as ligand atoms in the form of C=O chemical group in a bidentate oxalate ligand bites the metal cation in two places at a time produces a strong chelate compound to extract divalent metals from kidney and liver. This kind of chelation occurs to carboxylate oxygen and the adjacent hydroxyl group responding (i) a stable dodecahedral environment and (ii) bridging takes place through the coordinated carboxyl or the hydroxyl groups. Hence the chelating metallic compounds are found to be potential candidates for the removal of heavy metals in the order of trisodium citrate>disodium oxalate>sodium sulfate has been reported [5].

The metal-ligand binding should be hydrolytically stable due to the presence of the intermolecular H-bonds of water molecules [6]. In the water molecules ($\text{H}^{\delta+} - \text{O}_{\delta-} - \text{H}^{\delta+}$), the negatively charged oxygen forms two hydrogen bonds between two positively charged hydrogen atoms of neighboring molecules for the better nonlinear optical properties [7]. Moreover, in the metal ligand complex, the positive charge of the metal ion is

partially shared with the hetero donor atoms of hydrogen and oxygen present in the ligand and there may be π -electron delocalization over the whole chelating system [8].

In ionic doping, Na^+ is an important metal ion with defined ionic conductivity properties and is a versatile dopant. Further, Na^+ ion doping utilized for enhancing thermal stability of bimetallic dicarboxylate in the optoelectronic applications [9]. The optical conductivity in oxalate salts is due to the hydroxyl and carboxyl groups of the metal-oxalate matrix [10]. Optimized higher order optical conductivity on certain inorganic centro symmetric bimetallic oxalate and chloride have been suggested their potentiality for luminescent and nonlinear optical applications [11, 12].

The growth, structural stability and optical properties of potassium doped new copper oxalate crystal using the hydrothermal synthesis technique ($\text{K}_2\text{Cu}(\text{C}_2\text{O}_4)_2 \cdot 2\text{H}_2\text{O}$) has been reported [13]. Recently, some new coordination of ferrous and copper complexes have been reported on suitable antimicrobial activities [14]. Some copper complexes have also been shown biological properties in vitro [15].

Hence, in the present study, an attempt has been made to grow sodium doped copper oxalate crystals by a silica gel technique using single diffusion method. In order to prove the as-grown material is optically high, thermally stable and biologically active, the title compound has been subjected to various characterizations such as powder crystal XRD, FT-IR, UV-Vis-NIR, TGA, PL and antimicrobial screening activities.

II. Experimental

2.1 Materials and methods

The high-purity elements such as copper chloride (LOBA Chemie, 99.95 % Assay), sodium chloride (LOBA Chemie, 99.95 % Assay), oxalic acid (LOBA Chemie, 99.99 % Assay), and sodium metasilicate (LOBA Chemie, 99.9 % Assay) with AR grade were used as the starting materials in the single diffusion chemical reaction method at a temperature of 28°C . The X-ray diffraction (XRD) patterns of the prepared samples were recorded using an X'PERT-PRO diffractometer with Cu Ka (1.54060 \AA) at room temperature. The analysis was carried out at room temperature. The FTIR analysis was carried out using a PERKIN ELMER FTIR spectrometer by KBr pellet technique for deducing the presence of functional groups and the coordination of disodium copper oxalate dihydrate. The spectrum was recorded within the range of 400 cm^{-1} to 4000 cm^{-1} .

The optical characterization of sodium copper oxalate dihydrate crystal was carried with the help of a LAMBDA 35 UV Visible spectrophotometer. The transmission spectrum was traced to the range of 190 to 1100 nm. Thermal studies were carried out in the nitrogen atmosphere using the instrument SDT Q600 V20.9 in the temperature range from 20°C to 1100°C . TGA is used to determine the physical and chemical characteristics of materials, to determine degradation temperatures, absorbed moisture content of materials, the level of inorganic and organic components in materials and solvent residues. The weight of the NaCuOx crystal used for the measurement was from 3 to 4 mg and the heating rate was $10^\circ \text{C}/\text{min}$ under nitrogen medium.

The antimicrobial activity assayed against *Escherichia coli* (G-Ve) and *Aspergillus Niger*, according to agar well diffusion method. Nutrient agar (Merck, Germany) was used as solid media for preparing of nutrient plates while the Mueller Hinton broth was applied as liquid culture media in biological tests. Bacterial cultures such as *Escherichia coli* (G-Ve) and *Aspergillus Niger* were obtained from Eumic analytical Lab and Research Institute, Tiruchirappalli, Tamil Nadu, South India. Bacterial strains were maintained on Nutrient agar slants (Hi-media) at 4°C . Bacterial cultures were sub cultured in liquid medium (Nutrient broth) at 37°C for 8 h and further used for the test (10^5 - 10^6 CFU /ml). These suspensions were prepared immediately before the test was carried out.

2.2 Growth of $\text{Na}_4\text{Cu}_2(\text{C}_2\text{O}_4)_4 \cdot 4\text{H}_2\text{O}$

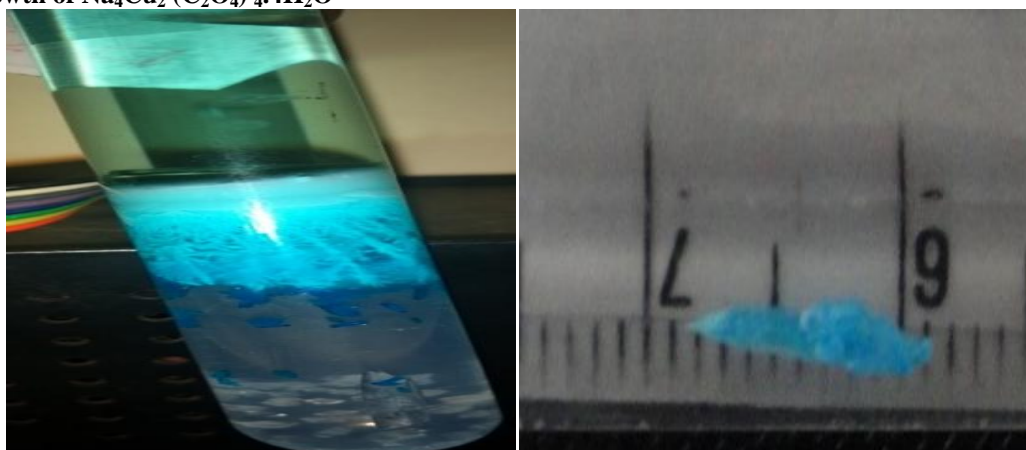
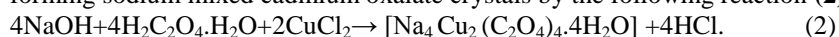


Figure1: sodium copper oxalate growth in gel medium. **Figure2:** size of the sodium copper oxalate crystal

The growth of sodium copper oxalate dihydrate crystal was carried out in silica gel media by adopting the single-diffusion technique is shown in **Fig.1**. The sodium copper oxalate dihydrate was prepared by gradual addition of cupric chloride (2 mmol in 10 ml of water) to a freshly prepared silica hydrogel [addition of sodium metasilicate solution (1.03 specific gravity) to oxalic acid (2 ml in 10 ml of water)], maintaining the pH at 3.5±0.2 - 4.5±0.2 and then left for a few days at room temperature for crystallization of the complexes. When sodium metasilicate goes into a solution, mono silicic acid is expected to be produced [16] according to the following reaction (1).



This sodium hydroxide is projected to react with oxalic acid, diffusing in a gel from the supernatant solution and forming sodium mixed cadmium oxalate crystals by the following reaction (2).



After passing 15 days, the sodium copper oxalate dihydrate $[\text{Na}_4\text{Cu}_2(\text{C}_2\text{O}_4)_4 \cdot 4\text{H}_2\text{O}]$ was obtained as suitable single crystals for optical and biological studies. **Table 1** shows the required growth parameters of the sodium copper oxalate crystal. The particle size of the sodium copper oxalate dihydrate was measured by $0.50 \times 0.55 \times 0.60 \text{ mm}^3$ using graphical method is shown in **Fig.2**.

Table1: Growth parameters of sodium copper oxalate crystals.

Process parameters	Single diffusion
Density of sodium metasilicate	1.04
pH of gel	4.5
Concentration of CdCl_2	1M
Concentration of NaCl	4M
Gel setting period	6 Days
Gel ageing	48 hours
Period of growth	10 Days
Temperature	Room temperature
Quality	Transparent, needle shaped
Size	$0.20 \times 0.25 \times 0.30 \text{ mm}^3$

III. Results And Discussion

3.1 Powder X-ray diffraction Analysis

The powder x-ray diffraction spectrum of sodium copper oxalate crystal is shown in **Fig.3**. The Powder XRD patterns identified that the formed crystals are in the single phase with good crystalline nature. The calculated lattice parameters of the as-grown crystal $[\text{Na}_2\text{Cu}(\text{C}_2\text{O}_4)_2 \cdot (\text{H}_2\text{O})_2]$ were $a=7.536 \text{ \AA}$, $b=9.473 \text{ \AA}$, $c=3.576 \text{ \AA}$, $\alpha = 81.90^\circ$, $\beta = 103.77^\circ$ and $\gamma = 108.09^\circ$ and it crystallized in the triclinic form of the P-1 space group through copper (II) atom lying on a center of symmetry has been reported [17].

The calculated hkl values of the sodium copper oxalate crystal with respect to the two theta values of the as-grown sodium copper oxalate crystals are shown in the **Table 2**. The diffraction peaks observed for sodium copper oxalate crystals are well agreed with the reported values [18] confirmed that the grown sodium copper oxalate crystal belongs to the triclinic system with space group P-1.

Table2: Calculated hkl parameters of sodium copper oxalate crystal

2 THEETA (degree)	hkl parameters
13.56	100
24.360	210
28.940	130
36.280	121
42.161	131
48.65	341
59.26	100
70.612	010

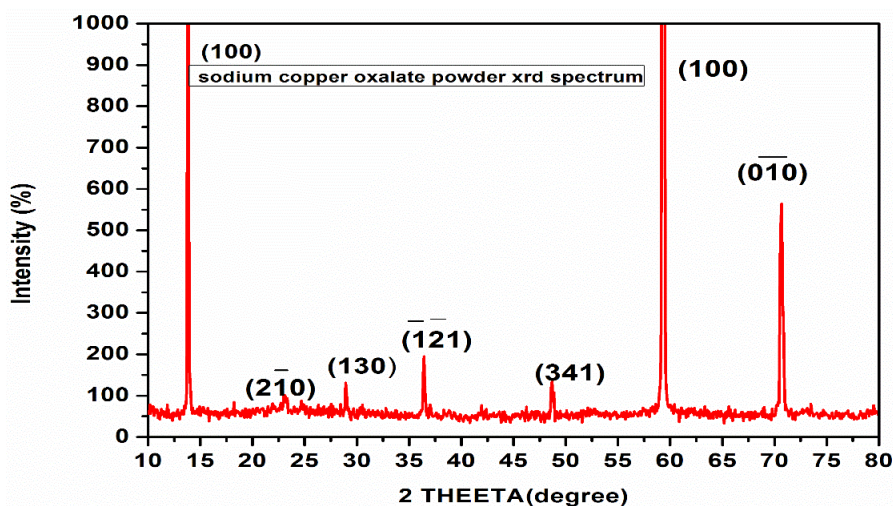


Figure3: Powder XRD spectrum of sodium copper oxalate dihydrate

3.2 FTIR Spectral analysis

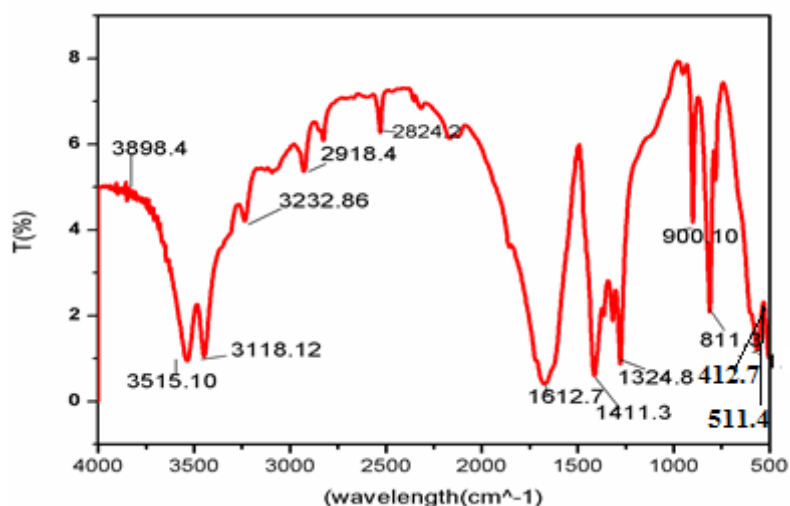


Figure 4: FTIR Spectrum of Oxalate-Ligand functional group assignments of NaCuOx crystal

The FTIR absorption spectrum of the as-grown sodium doped copper oxalate dihydrate single crystal was recorded from 400nm to 4000cm⁻¹ is shown in Fig.4. The broad envelope extending from 2824cm⁻¹ to 3898.4 cm⁻¹ are assigned to be due to the symmetric (O-H) and asymmetric (O-H) stretching modes of the water molecules. The phenomena observed in IR absorption spectra related to stretching ν_{sym} (O-H), (H-O... H), and ν_{asym} (O-H) bending vibrations are most characteristic. The ν (O-H), ν (COO)⁻ asymmetric stretching vibrations and one of the O-C=O deformation modes of vibrations were found at 3898.4cm⁻¹, 3515.10cm⁻¹, 3118.12 cm⁻¹ and 1324.8 cm⁻¹ which were standard for the optical and biological properties [19, 20] of the NaCuOx crystal. Undoubtedly, these phenomena are due to the changes in charge distribution, which may be related to electron delocalization. The broadband at 3515.10 cm⁻¹ in the spectra of the sodium copper oxalate complexes is assigned to the ν (OH) frequency of the coordinated H₂O. The strong band observed at 1612.7 cm⁻¹ in the spectra of the sodium copper oxalate ligand is a characteristic of the asymmetric stretching vibrations of C-O groups of the C₂O₄²⁻ ions together with the bending mode of water. The asymmetric stretching, vibration bands of carboxylate groups evolving at 1411.33 cm⁻¹ (C-H) is assigned to symmetric stretching of a COO⁻ group of the complex of sodium copper oxalate crystals. This shift can further be explained by the donation of electrons from the oxygen to the empty d-orbitals of the metal ions. [21]. The symmetric stretching vibration bands emerging from 900.10cm⁻¹ are assigned to (C-C) group. The bands below 800cm⁻¹ are due to the metal oxygen (M-O) bands. The charge transfer of the electron delocalization interaction, which is caused by charge transfer from occupied Na-O to vacant Cu-O, and the higher order coupled interactions. The number of absorption bands of the lower wave number region (<800 cm⁻¹) of sodium doped copper oxalate crystal was revealed the incorporation of sodium ions in the copper oxalate crystal lattice which formed additional metal – oxygen (Na-

O) bonding. The IR spectra of the assigned functional groups of as-grown sodium copper oxalate crystal have been well agreed with reported peaks of the pure copper oxalate crystals [22] is given in the **Table.3**.

Table3: Various modes of vibrations of oxalate-ligand functional group Assignments of NaCuOx crystal by FT-IR spectroscopy. (Band positions in (cm⁻¹)).

NaCuOx crystal band position(cm ⁻¹)	Assignment
3898.4m&3515.10w	v _{as} (H ₂ O)
3232.86w &3118.12w	v _s (H ₂ O)
2525.5 vw	v _{as} (COO)
1612.7vs	v _{as} (COO)
1411.33w	v _s (C-H)+ δ(O-C=O)
1324.8vs	v _s (CO)+ v _s (C-C)
900.10vs	δ (C-C)
811.3vs	δ(OCO)
412.7vs	v (Cu-O)
511.4 vs	v (Na-O)

V_s-very strong; s-strong; m-medium; w-weak; v_w-very weak; v_{as}-asymmetric stretching vibration; v_s ,symmetric stretching vibration; δ-deformation.

3.3 UV spectral studies

From the observed non-linear UV transmission vs. absorption spectral curves, the lower cut-off wavelength for sodium copper oxalate crystal was found to be 260.05 nm is shown in **Fig.5**. It is interesting to observe a strong, intense peak around 250-260 nm which is assigned to the oxalate group of the bimetallic oxalate crystal [23] has been reported. This special characteristic lower cut-off peak at 260.05 nm for the sodium copper oxalate crystal agreed to the n-π* transition due to a ligand-to metal charge transfer [24].

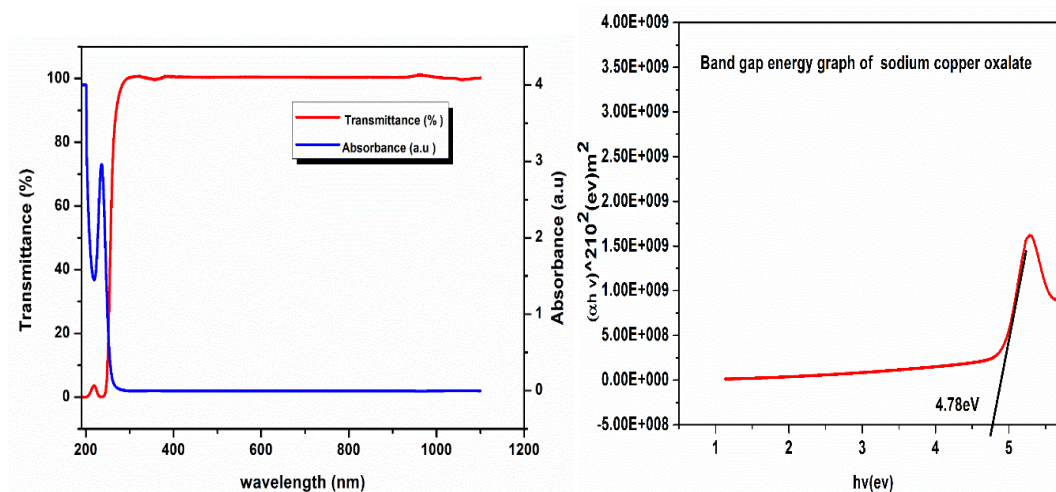


Figure 5 **Figure 6**

Figure 5: Observed non-linearity in the transmittance and absorbance curve of NaCuOx crystal.

Figure 6:observed non-linear band gap energy curve of NaCuOx crystal

In addition to that, the non-linear transmission curve was established to be 98.2% of sodium doped copper oxalate was observed in the wavelength region 245nm-1200nm. The calculated band gap energy of the as grown crystal is found to be 4.78 eV is shown in **Fig.6**.The wide range of band gap energy combined with the lower cut-off near 250nm, makes the usefulness of these materials for laser and device applications [25].The relation between the refractive index (n) and the energy gap (E_g) through some modified form of T.M Moss et al., and C.RamachandraRajaa, et al., [26, 27] were given by the equation (1),

$$E_g e^n = 36.3 \quad (1)$$

This relation holds true of energy gaps greater than 0 eV. The frequency or wavelength of refractive index is called dispersion. Dispersion is an important property for optical design and in the transmission of information. Further studies on the refractive index (n) and reflectance (R) of the crystals are calculated by using the expression (2), n=2.027; R=0.11525

$$R = \left(\frac{n-1}{n+1} \right)^2 \quad (2)$$

In the high photon energy region, the energy dependence on absorption coefficient was given by the equation (3),

$$\alpha = \frac{2.303}{t} \log \frac{1}{T} \quad (3)$$

Table4: Calculated optical parameters of as-grown NaCuOxcrystal

Compound	Wavelength (nm)	Energygap (eV)	Ref. index (n)	Reflectance (R)
NaCuOx	260.05	4.78	2.027	0.11525

Where ‘T’ is the transmittance and ‘t’ is the thickness of the crystal sample. Absorption coefficient ‘α’ suggests the occurrence of a direct band gap between the crystals which obeys the following equation (4) for high photon energies (hν) [28],

$$(ah\nu)^2 = A (E_g - h\nu) \quad (4)$$

where ‘α’ is the absorption coefficient, ‘h’ is the Plank’s constant, ‘A’ is a constant ‘ν’ is the frequency of the incident photon and ‘E_g’ is the optical band gap. The calculated high value of refractive index and low value of reflectance from the given **Table 4** confirmed that the grown crystal has wide transparency window and more transparent to transmit the light from 245 to 1100nm. As a result, the title crystal has been shown to be a useful material for the nonlinear optical and biological applications.

3.4 Thermal studies

3.4.1 DSC spectral analysis

The **Fig.7** shows the DSC curve of NaCuOx crystal upon heating in the temperature range from 20°C to 1100°C. The weight of the sample used for the measurement was 7.4990mg and the heating rate was 5min⁻¹ under a dry nitrogen gas flow of 100ml min⁻¹. At 115.05°C shows an endothermic process represents a transition from amorphous solid to a crystalline solid and results in a peak at the DSC signal is known as the Temperature (T_C) for NaCuOx. DSC is necessary to have well-characterized drug compounds in order to define processing parameters. For instance, if it is necessary to deliver a drug in the amorphous form, it is desirable to process the drug at temperatures below those at which crystallization can occur. The two large exothermic peaks were clearly seen on the DSC curve of NaCuOx crystal at 301.82°C and 346.95°C are represented as phase transitions from solid to gaseous states which informed the discharge of CO and CO₂ gas molecules due to the redox process which converted the hydrated crystalline Na₄Cu₂(C₂O₄)₄ salt into 2Na₂CuO_(s), 5CO_(g) and 3CO_{2(g)} [29].

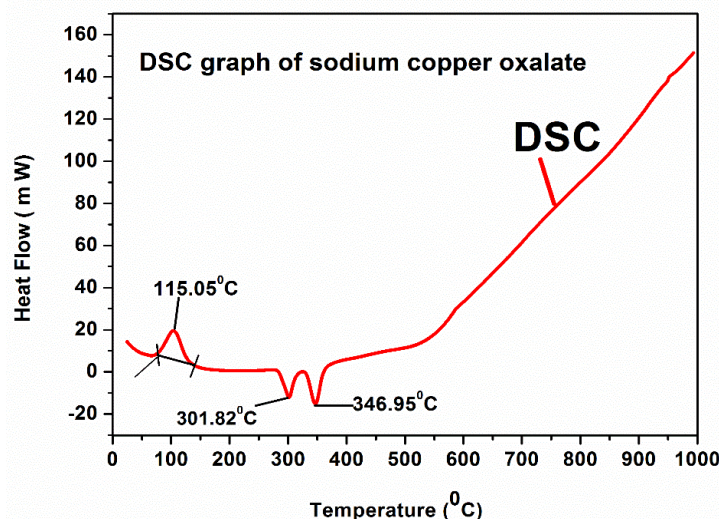


Figure 7: Observation of crystallization and phase transition temperatures of NaCuOx crystal by DSC spectrum

3.4.2 TGA/DTA analysis

The TGA/DTA thermogram of NaCuOx crystal shows that the heating in the temperature range from 20°C to 700°C for the weight of the sample used for the measurement was 7.4990mg and the heating rate was 5min⁻¹ under a dry nitrogen gas flow of 100ml min⁻¹. The first step of dehydration starts at 84.6°C and ends at 115.18°C, which shows the formation of anhydrous Na₄ Cu₂ (C₂O₄)₄ crystal from Na₄ Cu₂ (C₂O₄)₄.4H₂O sodium copper oxalate hydrate crystal, resulting in the weight loss of 11.21%. The weight loss takes place over a large temperature range (84.6°C –115.62°C) represents the melting point of the sample is shown in **Fig.8**.

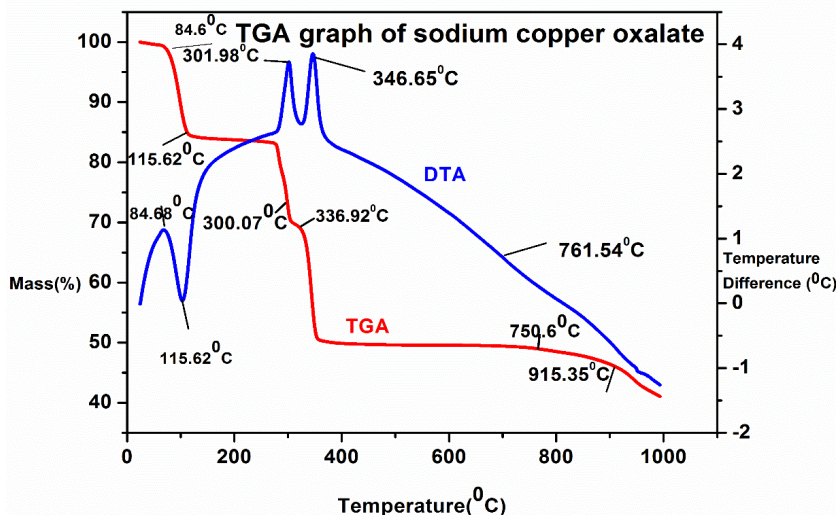


Figure 8: TGA/DTA thermo gram shows the different thermal decomposition stages of sodium copper oxalate crystal in the nitrogen atmosphere.

The calculated weight loss 11.20% in this temperature range is consistent with the weight of four water ($4\text{H}_2\text{O}$) molecules. The shoulder peaks at DTA after the main peak corresponds to the decomposition of the material. There is no phase transition till the material melts and this enhances the temperature range for the utility of the crystal for optical and biological applications. Generally, the exothermic and endothermic heat peaks in DTA curve, accompanied by decomposition at high temperature, are due to the formation and loss of gas, respectively.

The second and third steps represent the discontinuous decomposition of $\text{Na}_4\text{Cu}_2(\text{C}_2\text{O}_4)_4$ crystal into $[(2\text{Na}_2\text{O}_2)\cdot\text{Cu}_2\text{O}]$ sodium copper oxide in the temperature range of 200.02°C - 550.6°C with the discharge of 5CO and 3CO_2 gas molecules by showing the exothermic peak at 301.98°C with the corresponding 24.56% weight loss due to the emission of 5CO molecules and 23.47% weight loss at 346.65°C (300.07°C - 550.6°C) due to the discharge of 3CO_2 gas molecules for the production of sodium oxide copper oxide $[(2\text{Na}_2\text{O}_2)\cdot\text{Cu}_2\text{O}]$ has been found and consistent with the reported results[30,31]. The liberation of $\frac{1}{2}\text{O}_2$ gas molecules with the stable end product of sodium copper oxide ($2\text{Na}_2\text{OCuO}$) crystal during the fourth stage that extends up to the temperature range from 550°C - 700°C .

3.5 Photoluminescence spectrum

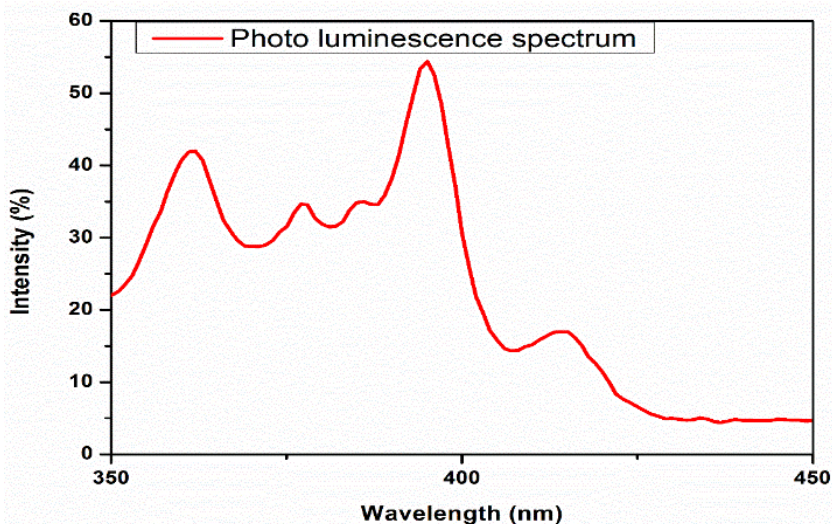


Figure 9: Photo luminescence spectrum shows the $n-\pi^*$ transmission of sodium copper oxalate crystal in the UV region

Presence of direct metal–metal interaction may be one of the important factors contributing to the photoluminescence, enhancing, shifting and quenching the luminescent emission of metal ligand by

complexation [32]. Thus, the photoluminescence of copper (II) complexes in the solid state at room temperature was examined. As shown in **Fig.9**, sodium copper oxalate complex exhibits photoluminescence in the solid state at room temperature with one of the emission peak maximized at 362.9 nm with excitation applied to 200nm-400 nm after exciting the sample of 250nm. The result indicates that the crystal has indigo fluorescence emission. The maximum intensity peak at 393.5 nm is attributed to $n-\pi^*$ transition of carbonyl group owing to result that the as-grown crystal has blue emission. The amount of splitting of the high intensity energy levels in NaCuOx is due to the diffusion of sodium⁺ ions into the ligand about Cu²⁺ metal ion. As a result, these metal complexes of ligand exhibit two excitation bands of 350nm -400nm of sharp absorption peaks at near UV regions.

3.6 Solubility

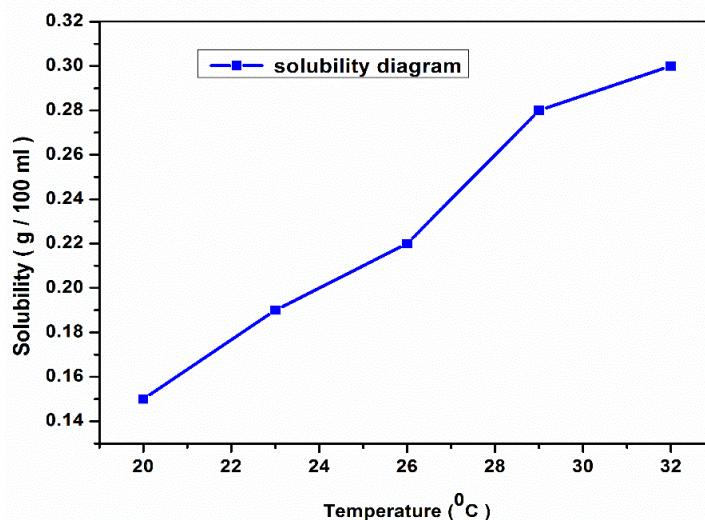


Figure 10: Solubility graph of sodium copper oxalate crystal at various temperatures.

Solubility is one of the factors of better biological activities [33] of the as-grown samples was proved by solubility test using deionized warm water as a solvent. The solubility of sodium copper oxalate was determined in the temperature range of 20 °C to 29 °C. Solubility studies were carried out in a constant temperature bath (CTB) with the cryostat facility with an accuracy of +0.01 K. The solution was stirred continuously for half an hour to achieve the stabilization. After attaining the saturation, the equilibrium concentration of the solute was analyzed gravimetrically. The same process was repeated and the solubility curves were observed to 0.05 g / 100 ml and 1.5 g /100 ml for as-grown crystals for different temperatures (**Fig.10**). It is observed from the curve that the solubility is found to increase with an increase in temperature for sodium copper oxalate dihydrate was due to the hydrogen bonding between sodium copper oxalate dihydrate and the soluble nature of sodium oxalate in water. This result showed the sustained activity of the as-grown sodium copper oxalate dihydrate sample in its chelate form and the improved solubility demands the sodium copper oxalate dihydrate crystal for further pharmaceutical research and applications.

3.7 Antimicrobial activity

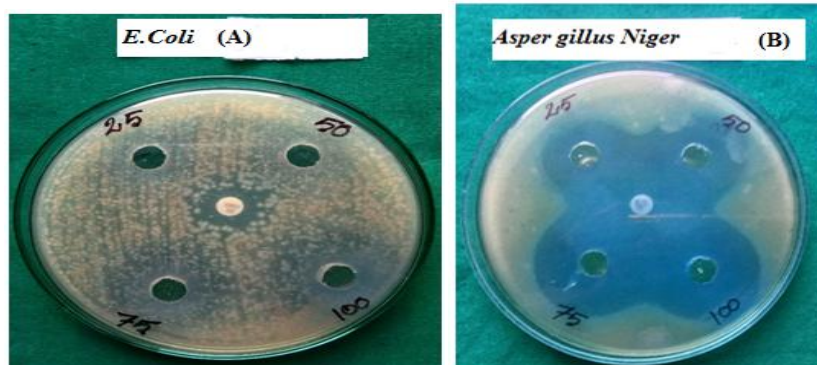


Figure 11(A)

Figure 11(B)

Figure 11(A): Antimicrobial activity of sodium copper oxalate against E. coli

Figure 11(B): Antimicrobial activity of sodium copper oxalate against Aspergillus Niger

Table 5: Antimicrobial activity of sodium copper oxalate crystal

Compound	Organism	Minimum Zone of Inhibition (mm) *				Control
		Concentration (µg / ml)				
		25	50	75	100	
Sodium copper oxalate	AspergillusNiger	28±0.2	30±0.3	33±0.3	36±0.4	18±0.1
Sodium copper oxalate	E.coli	20 ±0.1	24 ±0.2	27 ±0.4	30 ±0.3	20 ±0.3

*mean±SD

The antibacterial activity of the sodium copper oxalate dihydrate complex was tested against the Gram (–) *E. coli* and *Aspergillus Niger* organisms using double dilution method. An acceptable reason for this increase in bactericidal activity may be considered in the light of Overtone's concept and chelation theory [34]. According to Overtone's concept of cell permeability, the lipid membrane that surrounds cell favours the passage of only lipid soluble materials so that lipo solubility is an important factor which controls bactericidal activity. This increased lipophilicity due to the O-H...H and C-O bonds between the NaCuOx crystal enhance the $n \rightarrow \pi^*$ transition and also the penetration of the complexes about lipid membranes to block the metal binding sites in the bacterial enzymes. On chelation, the polarity of Cu (II) ion will be reduced to a greater extent due to the overlap between ligand orbital and partial sharing of the positive charge of the Cu (II) ion with donor groups [35]. **Fig. 11(A) & (B)** show, an increase in the concentration of test samples to give rise to more efficient effect of studied microorganisms. It has also been observed that quantitative assays gave MIC values in the range 25µl–100µl is shown in **Table.5** confirmed that concentration plays a vital role in increasing the degree of inhibition established that the results are superior to the previously published values [36].

IV. Conclusions

Optically active single crystal sodium copper oxalate crystal was obtained by single diffusion silica gel method. The crystal growth observations were revealed the dependence on morphology and the ultimate size of crystals on growth parameters like gel concentration, gel age, gel pH and the concentration of upper and lower reactants. The results of the structural analysis were indicating that the complex belongs to triclinic structure of P-1 space group. FT-IR band assignments were confirmed the presence of water of crystallization, expected metal-oxygen bonded groups and the oxalate phase transformation of as-grown copper (II) metal complexes of coordination compound. The DSC analysis revealed the gel-grown sodium copper oxalate crystal of the dehydration and decomposition temperatures in terms of their crystallization and the phase transition temperatures and also the high thermal stability of NaCuOx crystal for optical and biological applications. The optical behavior of NaCuOx crystal was studied by using UV-Vis-NIR spectrum and found to be 98.2% of the transmittance. The wide transparency was due to the localization of strong intermolecular hydrogen bonds and the $n \rightarrow \pi^*$ transition are the one of the key requirements for having an efficient optical conductivity character. The band gap energy together with wide optical efficiency and the significant ionic conductivity of the NaCuOx from UV and dielectric studies were designated the grown crystals could be a suitable material for the fabrication of optical devices. The NaCuOx complex showed good antimicrobial activity against *E.coli* (Gram-ve), *Aspergillus Niger* (Fungus) was attributable to the remarkable properties of its solubility, optical conductivity and semi polarity mechanisms.

Acknowledgements

The authors are also thankful to University Grants Commission, Grant no.F.NO: MRP-5808/15 (SERO/UGC) for providing financial support under Minor Research Project (MRP) scheme. We extend our heartfelt thanks to the Director, Central Electro Chemical Research Institute (CECRI), Karaikudi for XRD, PL, TGA/DTA&DSC characterization studies, Mr. Vincent, St. Joseph's college, Bishop Kaspar Central Instrumentation Facilities, Tiruchirappalli for UV & FT-IR studies, Dr. Senthil, Eumic research laboratory, SMS Hospital, Tiruchirappalli for Antimicrobial screening studies.

References

- [1]. Torres M.E, Lopez T, Peraza J, Stockel J, Yanes A.C. Structural and dielectric characterization of cadmium tartrate. *Journal of Applied Physics*. 1998; 84: 5729-32.
- [2]. Torres M.E, Yanes A.C, Lopez T, Stockel J, Peraza J.F, Characterization and thermal and electromagnetic behavior of gadolinium-doped calcium tartrate crystals grown by the solution technique. *J.crys.growth*. 1995; 156: 421-425.
- [3]. Thomas et al., Requirements for a GaAsBi 1 eV sub-cell in a GaAs-based multi-junction solar cell. *Semicond. Sci. Technol*. 2015; 30:094010 (6pp).
- [4]. Hodgkin son. A. Oxalic acid in biology and medicine. *Febs Letters*. Academic Press, London, 1977; 101:1-326.
- [5]. Atheer. A. M, Abdulqader M. A, Mohammed MosaJafaar. Studying of transition metal complexes containing oxalate ion with antibacterial activity. *International Journal of Scientific & Engineering Research*. 2015; 6:855-67.
- [6]. Namkanisorn A, Ghatak A, M. K. Chaudhury, K. Berry D.H, A kinetic approach to study the hydrolytic stability of polymer-metal adhesion. *J. Adhesion Sci. Technol*. 2001; 15:1725–45.

- [7]. Guido J. Reiss, Martin van Megen, and Frank, Hydrogenbonds and van der Waals forces as tools for the construction of a herringbone pattern in the crystal structure of hexane-1, 6-diaminium hexane-1, 6-diyl bis (hydrogen phosphonate). *Acta Crystallogr E Crystallogr Commun.* 2017; 73: 76–80.
- [8]. Singh Jadon S. C, Gupta N, Singh R V. Synthetic and biochemical studies of some hydrazine carbodithioic acid derivatives of dioxomolybdenum (VI). *Ind J Chem.* 1995; 34A: 733-6.
- [9]. Amuthambigai C, Mahadevan C.K, SahayaShajan X. Growth and characterization of bimetallic (Na and K) phthalate single crystals. *Appl. Phys A.* 2016; 122: 901 - 8.
- [10]. Schuster P, *The Hydrogen Bond—Recent Development in Theory and experiment.* North-Holland publishing company, Amsterdam. 1977; 89: 348–9.
- [11]. M. Narsimhulu, B.Rajub, A.Saritha, D.Narayana Rao, K. A. Hussain. A new room-temperature ultra violet emission material: $K_2 [Ni (C_2O_4)_2(H_2O)_2] \cdot 4H_2O$. *Physica B.* 2015; 472: 45–48.
- [12]. M Packiya raja M, S. Ravi Kumar S.M, R Srineevasan R, Ravisankar R, Synthesis, growth, and structural, optical, mechanical, electrical properties of a new inorganic nonlinear optical crystal: Sodium manganese tetrachloride (SMTC), *Journal of Taibah University for Science* 2017;11: 76–84L.
- [13]. Ai-Li Cui, Jing-Zhi Wei, Jin Yang, Hui-Zhong Kou. Controlled Synthesis of Two Copper Oxalate Hydrate Complexes: Kinetic versus Thermodynamic Factors. *Journal of Chemical Education.* 2009; 86(5):598-599.
- [14]. Prema P, Selvarani M, Evaluation of antibacterial efficacy of chemically synthesized copper and zerovalent iron nanoparticles. *Asian J Pharm Clin Res.* 2013; 6:222-7.
- [15]. Stevenson J, Barwinska-Sendral J, Tarrant E, Waldron K.J. Mechanism of action and applications of the antimicrobial properties of copper. *Microbial pathogens and strategies for combating them: Science, technology and education.* 2013; 1:468-479
- [16]. Daisy Selasteen F, Alfred Cecil Raj S, Alagappa Moses A, Synthesis and characterization in vitro antimicrobial and cytotoxicity testing of oxalic acid -derived cadmium chelating agents. *Int J Pharm Pharm Sci.* 2018; 10:80-6.
- [17]. Gleizes A, Maury F, and Galy J. Crystal Structure and Magnetism of Sodium Bis(oxalato)cuprate (II) Dihydrate, $Na_2Cu(C_2O_4)_2 \cdot 2H_2O$ Deductive Proposal for the Structure of Copper Oxalate, $CuC_2O_4 \cdot xH_2O$ ($0 < x < 1$). *Inorg. Chem.* 1980;19: 2014-8
- [18]. R. Polou, C. Triche, B. Barbier, G. Pitet. Sodium Copper Oxalate Dihydrate: $Na_2Cu (C_2O_4)_2 \cdot 2H_2O$ Synthesis, Characterization, Morphology and Optical Properties. *Powder Diffraction.* 1989; 4(1):14-18
- [19]. R.L. Frost, M.L. Weier, Raman spectroscopy of natural oxalates at 298 and 77 K. *J. Raman Spectrosc.* 2003; 34: 776-785.
- [20]. G.M. Begun, W.H. Fletcher, Vibrational spectra of aqueous oxalate ion. *Spectrochim. Acta.* 1963; 19: 1343-1349.
- [21]. Lewandowski W., Dasiewicz B., Koczon P., Skierski J., Teperek K. D., Swislocka R., Fuks L., Priebe W., Mazurek A.P. J. *Molecular Str.* 2002; 604: 189–193.
- [22]. A.S. Khan, T.C. Devore, Wilfred F. Reed. Growth of the Transition Metal Oxalates In Gels. *Journal of Crystal Growth.* 1976; 35:337-339.
- [23]. Varughese john, M.A.Ittyachen, K.S.Raju. Lanthanum-samarium oxalate: Its growth and structural characterization. *Bull. Mater. sci.* 1997; 20:1059-68
- [24]. K. Ambujam, K. Rajarajan, S. Selvakumar, I. VethaPotheher, Ginson P. Joseph, P. Sagayaraj, Growth and characterization of a novel NLO crystal bis-glycine hydrogen chloride, *J. Cryst. Growth.* 2006; 286: 440-444.
- [25]. Anthoni Praveen Menezes, A. Jayarama, SeikWengN, Synthesis, crystal growth and characterization of a D- π -A type novel organic nonlinear optical single crystal, *J. Cryst. Growth.* 2014; 402:130-137.
- [26]. T.S.Moss, Relations between the Refractive Index and Energy Gap of Semiconductors, *J. Phys. Stat. Sol (B).* 1985; 131: 415-427.
- [27]. C. RamachandraRajaa, G. Gokilab, A. Antony Joseph, Growth and spectroscopic characterization of a new organic nonlinear optical crystal: l-Alaniniumsuccinate, *spectrochimica Acta Part A.* 2009;72: 753–756.
- [28]. Tauc J, Grigorovici R. Vancu, Optical Properties and Electronic Structure of Amorphous Germanium, *Physica Status Solidi B.* 1966;15: 627-637.
- [29]. Christensen, A. N., Lebech, B., Andersen, N. H., & Grivel, J-C. (2014). The crystal structure of paramagnetic copper (ii) oxalate (CuC_2O_4): formation and thermal decomposition of randomly stacked anisotropic nano-sized crystallites. *Dalton Transactions.* 2014; 43(44): 16754-16768.
- [30]. Athare A. E, Nikumbh A .K, and Kolhe N. H. Direct Current Electrical Conductivity Study of the Thermal Decomposition of Copper (II) Monohydrate and Zinc (II) Oxalate Dihydrate. *Research Journal of Pharmaceutical, Biological and Chemical Sciences.* 2013; 4:110-127
- [31]. B B Parekh, P.M Vyas, Sonal R Vasant and M J Joshi. Thermal, FT-IR and dielectric studies of gel grown sodium oxalate single crystals. *Bull. Mater. Sci.* 2008; 31: 143–147.
- [32]. S.H. Rahaman, R. Ghosh, T.H. Lu, B.K. Ghosh, Chelating N,N' - (bis (pyridin-2-yl) alkylidene) propane-1,3-diamine pseudohalide copper(II) and cadmium(II) coordination compounds: Synthesis, structure and luminescence properties of $[M(bpap)(X)]ClO_4$ and $[M(bpap)(X)_2]$ [$M = Cu, Cd; X = N_3^-, NCS^-$]. *Polyhedron.* 2005;4:1525-1532.
- [33]. Athimoolam S, Sridhar B, Hydrogen bonding motifs, spectral characterization, theoretical computations and anticancer studies on chloride salt of 6-mercaptopurine: An assembly of corrugated lamina shows enhanced solubility. *J Molecular Structure.* 2015;1098: 332-41.
- [34]. Tweedy B.G. Plant Extracts with Metal Ions as Potential Antimicrobial Agents. *Phytopathology.* 1964; 55: 910-8.
- [35]. Jeyaprakash Dharma-rajaa, Paramasivam Subarea, Thirugnanasam, Esakkidurai, SuthaShobana, Coordination behavioural and bio-potent aspects of Ni (II) with 2-aminobenzamide and some amino acid mixed ligands – Part II: Synthesis, spectral, morphological, and pharmacological and DNA interaction studies. *Spectrochimica Acta Part A.* 2014; 132: 604-714
- [36]. Zahid H, Chohan M. Ni (II), Cu (II) And Zn (II) metal chelates with some thiazole derived Schiff-bases. Their synthesis, characterization and bactericidal properties. *Journal of Metal-Based Drugs.* 1999; 6:75–80. DOI: 10.1155/MBD.1999.75

: F. Daisy Selasteen "Growth and Characterization in Vitro Antimicrobial Activity of Oxalic Acid -Derived Copper Complex of Non Linear Optical Crystal "IOSR Journal of Applied Physics (IOSR-JAP) , vol. 10, no. 5, 2018, pp. 16-25.